DOI: 10.1002/cbic.200600261

Systematic Regulation of the Enzymatic Activity of Phenylacetaldoxime Dehydratase by Exogenous Ligands

Katsuaki Kobayashi,[a] Minoru Kubo,[a] Shiro Yoshioka,[a] Teizo Kitagawa,[a] Yasuo Kato,[b] Yasuhisa Asano,*[b] and Shigetoshi Aono*[a]

Phenylacetaldoxime dehydratase from Bacillus *sp. OxB-1 (OxdB) contains a heme that acts as the active site for the dehydration reaction of aldoxime. Ferrous heme is the active form, in which the heme is five coordinate with His282 as a proximal ligand. In this work, we evaluated the functional role of the proximal ligand for the catalytic properties of the enzyme by "the cavity mutant technique". The H282G mutant of OxdB lost enzymatic activity, although the heme, which was five coordinate with a water molecule (or OH^-) as an axial ligand, existed in the protein matrix. The enzymatic activity was rescued by imidazole or pyridine derivatives that acted as the exogenous proximal ligand. By changing the electron-donation ability of the exogenous ligand with different substituents, the enzymatic activity could be regulated systematically. The stronger the electron-donation ability of the exogenous ligand, the higher was the restored enzymatic activity. Interestingly, H282G OxdB with 2-methyl imidazole showed a higher activity than the wild-type enzyme. Kinetic analyses revealed that the proximal His regulated not only the affinity of substrate binding to the heme but also the elimination of the OH group from the substrate.*

Introduction

Phenylacetaldoxime dehydratase from *Bacillus* sp. strain OxB-1 (OxdB) catalyzes the dehydration reaction of *Z*-phenylacetaldoxime (PAOx) to form phenylacetonitrile (PAN) (Scheme 1),

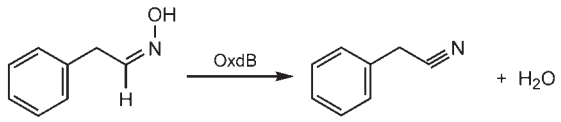

Scheme 1. The dehydration reaction of PAOx catalyzed by OxdB.

which is involved in the nitrile metabolism pathway in this bacterium.[1,2] This enzyme is an example of a heme protein that physiologically catalyzes the dehydration reaction. Although the redox chemistry of the heme is usually adapted for the catalysis by heme enzymes, this is not the case for OxdB. The primary role of the heme in OxdB is to tether the substrate with the proper configuration for catalysis.[3]

Mansuy and his colleagues have proposed a reaction mechanism for the dehydration of aldoxime catalyzed by iron porphyrins[4] or cytochrome P450.[5] In their proposed mechanism, aldoxime binds to the ferrous heme iron atom through the nitrogen atom of aldoxime at first, and then a water molecule is eliminated from the heme-bound substrate by acid–base catalysis. Aldoxime dehydratase, which physiologically catalyzes the dehydration of aldoxime, also adopts the above mechanism.[3,6] We have reported that the ferrous heme in OxdB binds PAOx through coordination of its nitrogen atom.[3] In the case of aldoxime dehydratase, a histidine residue acts as a catalytic residue in the distal heme pocket.[3,6] Recently, resonance Raman spectroscopy has revealed a reaction intermediate containing a Fe^{4+}=N–R moiety with a double bond between the iron atom and the nitrogen atom of aldoxime in OxdA, an aldoxime dehydratase from *Pseudomonas chlororaphis* B23;[7] this is also a postulated intermediate in the mechanism of Mansuy and co-workers.

Site-directed mutagenesis has revealed that His299 is the proximal ligand of the heme in OxdA.[6] H299A OxdA loses the heme, which results in the loss of the enzymatic activity.[6] While these results indicate that the proximal His is important to tether the heme in aldoxime dehydratase, it is not obvious whether this residue plays a further role for the regulation of the enzymatic activity. Simple site-directed mutagenesis on the proximal His is not very useful to answer this question. A

[a] *Dr. K. Kobayashi, Dr. M. Kubo, Dr. S. Yoshioka, Prof. T. Kitagawa, Prof. S. Aono*
Okazaki Institute for Integrative Bioscience
National Institutes of Natural Sciences
5–1 Higashiyama, Myodaiji, Okazaki 444-8787 (Japan)
Fax: (+81) 564-59-5576
E-mail: aono@ims.ac.jp

[b] *Prof. Y. Kato, Prof. Y. Asano*
Biotechnology Research Center, Faculty of Engineering
Toyama Prefectural University
5180 Kurokawa, Imizu, Toyama 939-0398 (Japan)
Fax: (+81) 766-56-2498
E-mail: asano@pu-toyama.ac.jp

Supporting information for this article is available on the WWW under http://www.chembiochem.org or from the author.

heme is easily lost by the mutation of the proximal ligand, as shown in H299A OxdA. Even if an amino acid such as Cys or Tyr is introduced as a possible proximal ligand instead of His, Cys or Tyr will hardly coordinate to a ferrous heme in the mutant protein.

A way to answer the above question would be "the cavity mutant technique".[8,9] This technique is a unique method to elucidate the functional roles of the proximal ligand, in which the proximal ligand is mutated to Gly to make a cavity accommodating an external ligand in the proximal heme pocket. The heme is reconstituted in the heme pocket of a cavity mutant by introducing an external ligand that can substitute for the endogenous proximal ligand. Imidazole (Im) and its derivatives are usually used to substitute for His. This technique was applied to myoglobin (Mb) at first and was then extended to heme oxygenase (HO), cytochrome *c* peroxidase (CCP), and horseradish peroxidase (HRP) to elucidate the roles of the proximal His in these proteins.[8–23] It allows the study of the functional effects of the different electronic properties of the proximal heme ligand by changing a substituent of the exogenous ligand.

In this paper, we report the application of the cavity mutant technique to OxdB to elucidate the functional role of the proximal His for the catalysis of the dehydration of aldoxime. We have characterized the biochemical and biophysical properties of the cavity mutant of OxdB with and without various exogenous ligands. The enzymatic activity of the cavity mutant of OxdB could be systematically regulated by changing the electron-donation ability of the external ligand. We discuss the electronic effects of the proximal ligand on the basis of the kinetic analyses.

Results and Discussion

In this work, the cavity mutant of OxdB (H282G OxdB), in which the proximal histidine of the heme (His282) is replaced by Gly, was prepared to elucidate the functional role of the proximal ligand for the enzymatic properties of OxdB. When the proximal ligand of a heme protein is mutated to Gly, the expressed mutant (the cavity mutant) generally loses the heme to be expressed as the apo form. In some cases, however, the heme can be reconstituted in the apoprotein in vitro by adding imidazole or imidazole derivatives.[12] In the case of Mb, a holo form of the cavity mutant (H93G Mb) can also be obtained in vivo when H93G Mb is expressed and purified in the presence of Im.[8,9]

H282G OxdB was obtained as a mixture of the apo and holo forms when it was expressed, even in the absence of Im. The content of the holo form increased when the recombinant *Escherichia coli* cells were grown in the presence of Im (data not shown). Once a heme was introduced into H282G OxdB, it was not released from the protein matrix, even though Im was released from the protein during purification in the absence of Im (see below). This property of H282G OxdB is different from that of H93G Mb, in which the heme reconstituted in the presence of Im is released from the protein by decreasing the concentration of Im. These results suggest that the flexibility of the heme pocket is different between H282G OxdB and H93G Mb.

OxdB shows 32–33% identity and 50–53% similarity of the amino acid sequence when compared with OxdA and other Oxds.[24,25] Although the homology is relatively high, the properties of the proximal histidine mutants are different between OxdA and OxdB. While the heme is completely lost in OxdA upon the mutation of the proximal histidine,[6] the heme is retained in H282G OxdB. These results suggest that the heme environmental structure and/or the flexibility of the heme pocket are different between OxdA and OxdB. However, the molecular structures of OxdA and OxdB, which are not available yet, are required to discuss these points in detail.

H282G OxdB showed a Soret band at 402 nm and peaks at 490, 537, and 601 nm in the Q-band region (pH 7.0; Figure S1 in the Supporting Information). Ferrous H282G OxdB showed a Soret band at 425 nm and peaks at 552 and 588 nm in the Q-band (Figure S1 in the Supporting Information). While these spectra are quite different from those of wild-type (WT) OxdB, they are very similar to those of the heme-reconstituted H93G Mb[17] and heme-bound H25A HO,[18] in which the heme is five coordinate with a water molecule (or OH^-) as the axial ligand.

The coordination structure and the spin state of the heme in H282G OxdB were studied by resonance Raman spectroscopy. In the high-frequency region of the resonance Raman spectra, ferric H282G OxdB showed ν_2, ν_3, and ν_4 bands at 1575, 1490, and 1373 cm^{-1}, respectively (Figure 1 A), which is typical of a

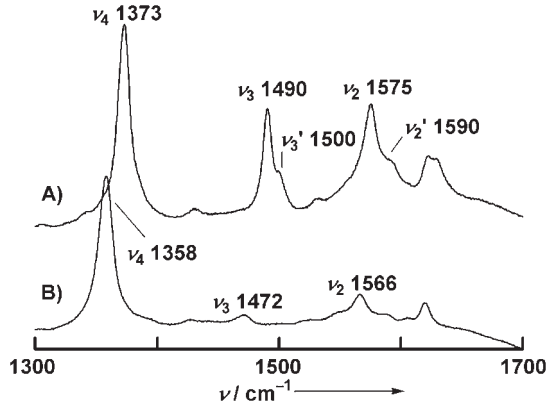

Figure 1. Resonance Raman spectra of A) ferric and B) ferrous H282G OxdB.

five-coordinate high-spin (5C/HS) heme. Minor bands due to ν_2' and ν_3' were observed at 1590 and 1500 cm^{-1}, respectively, thereby suggesting the existence of a 5C/HS heme with a different conformation. WT OxdB shows these bands at $\nu_2 = 1563$, $\nu_3 = 1479$, and $\nu_4 = 1369$ cm^{-1}, which is typical of a six-coordinate high-spin (6C/HS) heme. These results indicate that ferric H282G OxdB has a 5C/HS heme, whereas WT OxdB has a 6C/HS heme. Ferrous H282G OxdB showed these marker bands at $\nu_2 = 1566$, $\nu_3 = 1472$, and $\nu_4 = 1358$ cm^{-1}, values which are typical of a 5C/HS heme (Figure 1 B).

Although the Raman band due to the Fe–His stretching mode is observed at 223 cm^{-1} in ferrous WT OxdB,[26] the Fe–His band disappeared in H282G OxdB (Figure 2 A). These

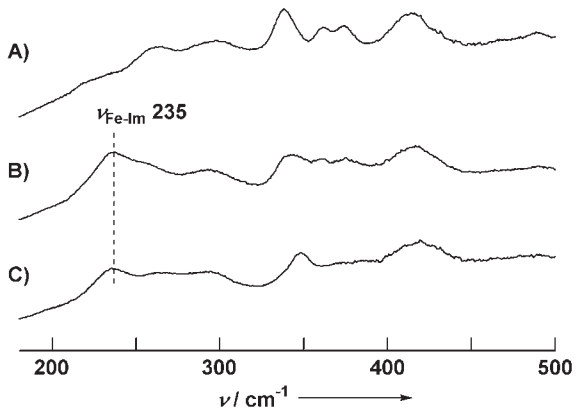

Figure 2. Resonance Raman spectra of ferrous H282G OxdB A) in the absence of Im and in the presence of B) 0.8 mM and C) 80 mM Im, measured in the low-frequency region.

results indicate that the heme in ferrous H282G OxdB is five-coordinate with a water molecule (or OH^-) as the axial ligand, as is the case with H93G Mb and heme-bound H25A HO.

The addition of imidazole to ferrous H282G OxdB resulted in a shift of the Soret band from 425 nm to 427 nm, which suggests that Im bound to the heme (Figure S2 in the Supporting Information). The resonance Raman spectra of ferrous H282G OxdB also changed upon addition of Im (Figure 2). In the low-frequency region, a signal due to the Fe–Im stretching mode was observed at 235 cm^{-1} upon addition of Im to ferrous H282G OxdB. The appearance of the band at 235 cm^{-1} clearly indicates the formation of an Im-bound, five-coordinate heme upon addition of Im to ferrous H282G OxdB. As described below, similar five-coordinate hemes were formed upon addition of imidazole derivatives (Im(X)) or pyridine derivatives (Py(X)). The frequencies of the Fe–ligand stretching mode are summarized in Table 1. Although the enzymatic activity was restored by Im(X) or Py(X), as described below, no correlation was observed between the $\nu_{Fe\text{–}ligand}$ frequency and the restored activity of H282G OxdB.

The intensity of the signal due to the Fe–Im stretching mode decreased beyond a maximum with increasing [Im] (Figure 2). These results indicate the formation of a six-coordinate heme with bis-Im binding upon increasing [Im], which was confirmed by the resonance Raman spectra in the high-frequency region.

In the high-frequency region, new ν_2, ν_3, and ν_4 bands appeared at 1583, 1495, and 1374 cm^{-1}, respectively, when [Im] was increased (Figure 3B and C). These bands are typical of a six-coordinate low-spin (6C/LS) heme. Similar changes on the resonance Raman spectra were also observed when other Im derivatives were added. The results can be explained as follows. When Im is added to ferrous H282G OxdB, an Im replaces the water coordinated to the heme to form an Im-bound 5C/HS heme. As [Im] increases, a second Im is coordinated to the heme to form a bis-Im-bound heme.

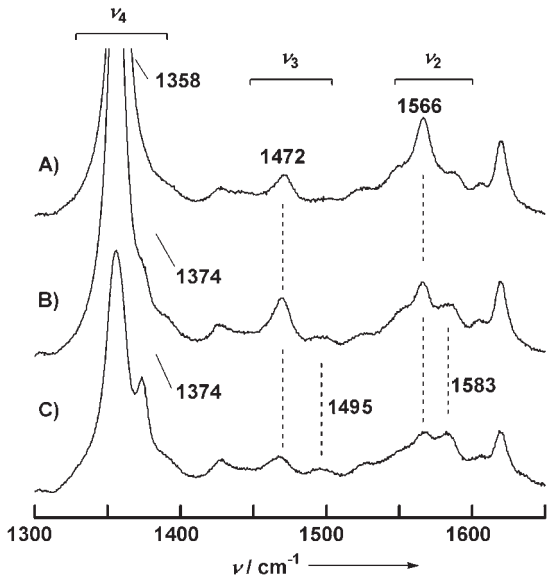

Figure 3. Resonance Raman spectra of ferrous H282G OxdB A) in the absence of Im and in the presence of B) 0.8 mM and C) 80 mM Im, measured in the high-frequency region.

The specific activity of ferrous H282G OxdB was 49 s^{-1} based on the heme concentration, which was about 2% of the activity of wild-type OxdB (2.3×10^3 s^{-1}[3]). These results indicate that the proximal histidine plays a critical role for the dehydration reaction of aldoxime. The electronic absorption spectrum of H282G OxdB was changed upon addition of PAOx, in that the Soret peak of ferrous H282G OxdB shifted from 425 nm to 423 nm; this was accompanied with a decrease in the peak intensity. These results suggest that PAOx bound to the heme even in the absence of the proximal His. The absence of the proximal His may cause the loss

Table 1. The Raman bands of $\nu_{Fe\text{–}ligand}$ and the kinetic parameters of H282G OxdB in the presence of various exogenous ligands.

	pK_a	Hammett constant σ	$\nu_{Fe\text{–}ligand}$ [cm^{-1}]	K_m [mM]	k_{cat} [s^{-1}]
Im(2Me)	7.92		219	1.10	4.3×10^3
Im(4Me)	7.57		220	0.47	2.6×10^3
Im	7.04		235	0.76	3.8×10^3
Im(1Me)	7.02		223	0.78	3.9×10^3
wild-type	5.97 (histidine)		223	0.70	3.2×10^3
Im(1Vi)	5.69		213	2.52	1.9×10^3
Py(4OMe)		−0.268	198	1.64	9.6×10^2
Py(4Me)		−0.170	198	0.67	5.4×10^2
Py		0	211	0.38	3.1×10^2
Py(4Cl)		0.227	190	0.46	1.0×10^2
Py(4Ac)		0.500	193	0.48	84

of the electronic effect from the proximal ligand and/or a change in the location of the heme in the protein matrix that results in the incorrect orientation of the heme-bound PAOx toward the catalytic residues.

The addition of Im to ferrous H282G OxdB restored the enzymatic activity. The activity gradually increased with increasing [Im] and then reached a constant value at high [Im] values (Figure 4). The restored activity finally reached $3.5\times10^3\ s^{-1}$,

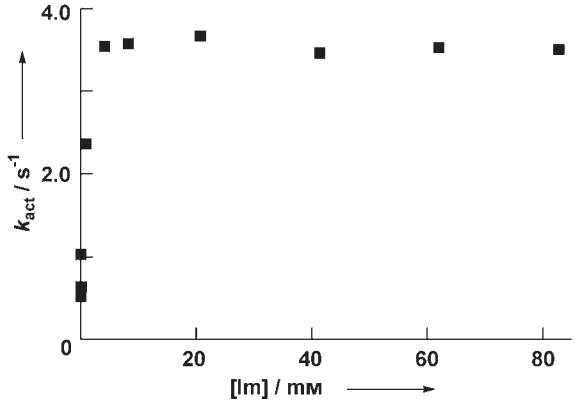

Figure 4. Graph indicating chemical rescue of the enzymatic activity of ferrous H282G OxdB with Im.

which was higher than that of ferrous WT OxdB. These results indicate that the heme–Im complex occupies the same position as the heme does in WT OxdB and that PAOx binds to the distal side of the heme in which the catalytic residues exist.

As the dehydration reaction of aldoxime proceeds through substrate coordination to the heme,[3–6] the heme should have a vacant site to bind the substrate for catalysis. However, a bis-Im-bound heme was formed with increased [Im] values, as described above. These results suggest that Im may be a competitive inhibitor for PAOx dehydration with H282G OxdB. If both of the imidazoles are tightly bound to the heme even in the presence of PAOx, enzymatic activity will not be observed because of the inability of the substrate to bind to the heme. However, this was not the case. Inhibition of the enzymatic activity by Im was not observed, as shown in Figure 4. The activity of H282G OxdB increased with increasing [Im] values and then reached a constant value. These results indicate that the second Im bound to the ferrous heme is easily replaced by PAOx during catalysis and that the Im retained as the axial ligand is located at the proximal position during catalysis. Imidazole was not a competitive inhibitor under the experimental conditions.

The activity of H282G OxdB could be systematically regulated by changing the electron-donation ability of the exogenous ligand. 2-Methylimidazole (Im(2Me)), 4-methylimidazole (Im(4Me)), imidazole (Im), 1-methylimidazole (Im(1Me)), and 1-vinylimidazole (Im(1Vi)) were used for the reconstitution of H282G OxdB; The pK_a values of these compounds, which correlate to the electron-donation ability, are 7.92, 7.57, 7.04, 7.02, and 5.69, respectively. All Im derivatives were effective for the restoration of the enzymatic activity of ferrous H282G OxdB. The dependence of the restored activities on the concentrations of the Im derivatives showed saturation curves, as was observed for Im (Figure S3 in the Supporting Information).

The restored activity of ferrous H282G OxdB finally reached constant values of 3.6×10^3, 2.1×10^3, 3.5×10^3, 3.4×10^3, and $1.5\times10^3\ s^{-1}$ for Im(2Me), Im(4Me), Im, Im(1Me), and Im(1Vi), respectively (Figure S3 in the Supporting Information). Interestingly, Im(2Me), which has the highest pK_a value among these Im derivatives, induced the highest restored enzymatic activity. These results implied that stronger electron donation of an exogenous ligand caused higher enzymatic activity of the cavity mutant.

To discuss in detail the effect of the electron-donation ability of the exogenous ligand on the enzymatic activity, we did kinetic analyses for H282G OxdB/Im(X). The kinetic parameters were determined to be 0.76 mM and $3.8\times10^3\ s^{-1}$ for the Michaelis constant (K_m) and the rate constant of catalysis (k_{cat}), respectively, in the case of H282G OxdB/Im. The kinetic parameters for H282G OxdB with other Im derivatives are summarized in Table 1.

As shown in Figure 5A, a correlation between the k_{cat} and pK_a values of Im(X) in which the k_{cat} value increased along with the increasing pK_a value of Im(X)was observed, except with Im(4Me). These results suggest that electron donation from an exogenous ligand accelerates the elimination of the OH group of PAOx to generate a water molecule. While there was a correlation between the k_{cat} and pK_a values, the correlation between the K_m and pK_a values was not obvious (Figure 5B). This might be partly due to a steric effect of the Im(X). In the series

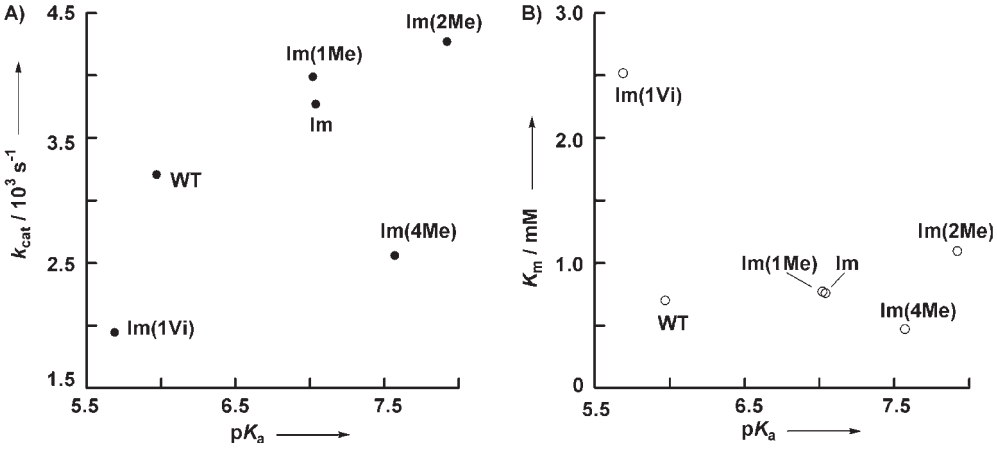

Figure 5. Dependence of the pK_a value on the A) k_{cat} and B) K_m values of H282G OxdB/Im(X).

of the imidazole derivatives used in this study, the substituents are located at different positions on the imidazole ring. The difference in the steric interactions among the heme, the imidazole derivatives, and the protein matrix might affect the k_{cat} and K_m values of H282G OxdB/Im(X).

In order to avoid the steric effects observed in H282G OxdB/Im(X) system, we employed 4-substituted pyridine (Py(X)) instead of Im(X) as an exogenous ligand. Thereby, we could evaluate the effect of the electron donation from the exogenous ligand on the enzymatic activity without considering the steric effects. Pyridine derivatives have another advantage for the analyses, in that the substituent effects of aromatic compounds can be analyzed by the Hammett rule. We used the pyridine derivatives 4-methoxypyridine (Py(4OMe)), 4-methylpyridine (Py(4Me)), pyridine (Py), 4-chloropyridine (Py(4Cl)), and 4-acetylpyridine (Py(4Ac).

The enzymatic activity of H282G OxdB was also restored by these pyridine derivatives, although the restored activity was lower than that of WT OxdB. The kinetic parameters of H282G OxdB/Py(X) are summarized in Table 1. The more electron-donating ligands showed higher k_{cat} values, which was consistent with the results with Im derivatives.

The dependence of the k_{cat} value on the Hammett constant (σ) is shown in Figure 6B. The k_{cat} values showed a linear correlation with the Hammett constants. The negative slope of the correlation plot indicates that electron donation from the exogenous ligand stabilizes the cationic transient state proposed previously.[4,5] Electron donation from the proximal Py(X) enhances the electron density of the heme iron to promote π back donation from the dπ orbital of the low-spin Fe^{2+} in the heme to the π^* orbital of the C=N bond in the PAOx. This π back-donation effect seems to be predominant for the regulation of the k_{cat} value and to enhance the elimination of the OH group as a water molecule. These results suggest that elimination of the OH group from the heme-bound PAOx is the rate-limiting step.

The dependence of the K_m value on the Hammett σ is shown in Figure 6A. Two different linear correlations were observed with negative and positive slopes for (Py(4OMe), Py(4Me), and Py) and (Py, Py(4Cl), and Py(4Ac)), respectively. The substrate binding to the heme is thought to be regulated by a combination of σ donation and π back donation, as discussed below. PAOx can work as either a σ-donor ligand or a π-acceptor ligand. As the electron density of the heme iron increases, the σ bonding of PAOx becomes disadvantageous because of Coulombic repulsion. Instead, the π back bonding becomes advantageous with increasing electron density of the heme iron, which is an advantage for PAOx binding to the heme.

In the series of Py(X) with electron-donating substituents, the more electron-donating Py(X) compounds showed higher K_m values, thereby suggesting that the σ bonding effect predominantly controls the K_m value in this series of Py(X). In the case of Py, Py(4Cl), and Py(4Ac), the K_m value increased with the increasing of Hammett σ. In the series of Py(X) with electron-withdrawing substituents, the π back-bonding effect seems to become apparent, in that the K_m value increases as the π back bonding becomes weaker. These results suggest that the appropriate balance of electron donation from the proximal ligand exists in OxdB to regulate the affinity for substrate binding.

Conclusion

We prepared the cavity mutant of OxdB (H282G OxdB) and showed that this cavity mutant held a heme that was five-coordinate with a water (or OH^-) as an axial ligand. While H282G OxdB was inactive for the dehydration of PAOx, addition of exogenous Im or Py derivatives to H282G OxdB restored the enzymatic activity. Although a bis-Im-bound heme was formed at higher Im concentrations, PAOx replaced the second Im that bound to the heme at the distal heme pocket during catalysis. The restored activity of H282G OxdB could be controlled systematically by changing the electron-donation ability of the exogenous Im or Py derivatives. The more electron-donating ligands afforded higher enzymatic activity of H282G OxdB. In the case of H282G OxdB/Im(2Me), the restored activity was 1.6-fold higher than that of WT OxdB. To our knowledge, this is the first example of a cavity mutant of a heme enzyme that shows a higher activity than the wild-type enzyme. Kinetic analyses revealed that an increase in the electron density of

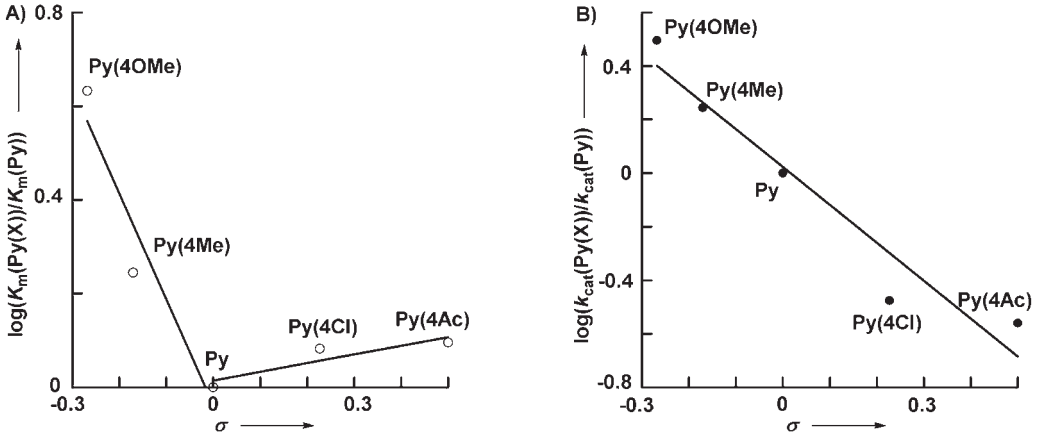

Figure 6. Hammett plots of the kinetic parameters of H282G OxdB/Py(X). The diagram of A) K_m versus the Hammett constant σ and B) k_{cat} versus the Hammett constant σ.

the heme iron accelerated the reaction by increasing the k_{cat} value, while the K_m value also increased.

Experimental Section

Site-directed mutagenesis was performed with the Quick Change site-directed mutagenesis kit (Stratagene). Amino-terminal His_6-tagged H282G OxdB was expressed in *E. coli* JM109 under the control of the *lac* promoter in pUC18. *E. coli* cells were grown at 37 °C in terrific broth medium containing ampicillin (100 μg mL^{-1}) and imidazole (10 mM). Isopropyl-β-D-thiogalactopyranoside (1 mM) and 5-aminolevulinic acid (1 mM) were added after 4 h of the cultivation, and then the cultivation was continued at 25 °C for 60 h. The cells were harvested by centrifugation and stored at −80 °C until use.

All purification procedures were performed at 4 °C, and H282G OxdB was purified as follows. *E. coli* cells were resuspended in 50 mM potassium phosphate buffer (pH 7.0) containing NaCl (300 mM). The suspended cells were disrupted by sonication and centrifuged to obtain a cell-free crude extract. The cell-free extract was loaded on a Co^{2+}-charged metal-ion-chelating (Talon) column. After washing of the column with potassium phosphate buffer (50 mM, pH 7.0) containing NaCl (300 mM), adsorbed proteins were eluted from the column with potassium phosphate buffer (50 mM, pH 7.0) containing imidazole (50 mM). The fractions containing OxdB were pooled and subsequently purified by using a Superdex 200 column with potassium phosphate buffer (50 mM, pH 7.0).

The electronic absorption spectra were measured on an Agilent 8453 UV–visible spectrometer. The resonance Raman spectra were measured with a 75–cm single spectrometer (SPEX750 M, Jovin Yvon) equipped with a 2400 groove mm^{-1} holographic grating and a liquid-nitrogen-cooled CCD detector (Spec10:400B/LN, Roper Scientific). The excitation wavelengths were 413.1 and 428.7 nm for ferric and ferrous OxdB, respectively. Continuous wave laser lights at 413.1 and 428.7 nm were obtained from a krypton-ion laser (BeamLok2060, Spectra Physics) and a diode laser (58-BTLR010, Melles Griot), respectively. The laser power was adjusted to ≈10 mW at the sample point. The sample cell was rotated at 2000 rpm. The Raman shifts were calibrated with indene and CCl_4, which provided an accuracy of ±1 cm^{-1} for well-defined Raman bands. The enzyme concentrations were adjusted to 12 mM. All resonance Raman spectra were measured at room temperature.

The enzymatic activity of OxdB was determined by the formation rate of the reaction product PAN. The reaction was carried out under anaerobic conditions. A typical reaction mixture for the assay contained the following components: potassium phosphate buffer (50 mM, pH 7.0, total volume of 500 μL) containing Im(X) or Py(X) (80–100 mM for the kinetic studies), solution of PAOx in *N*,*N*-dimethylformamide (50 μL of 100 mM solution), sodium dithionite (50 μL of 20 mM solution), and H282G OxdB (5 μL; 0.15–0.30 and 1.5–3.0 pmoles for Im(X) and Py(X), respectively). The buffer solution containing the substrate and Im(X) (or Py(X)) in a sealed tube with a rubber septum was degassed by a vacuum pump, and then dithionite solution was added under a nitrogen atmosphere. The reaction was started by injecting OxdB. The reaction was carried out at 30 °C. For product analysis, 200 μL of the reaction mixture were withdrawn and poured into the same amount of phosphoric acid (0.5 M) to quench the reaction. The reaction product was analyzed and monitored at 254 nm with an HPLC system (JASCO, pump; PU-2080 plus, UV/Vis detector; UV-2075 plus, column thermostat; CO-2060plus) with an octadecylsilyl column (4.6×150 mm) operating at a flow rate of 1.0 mL min^{-1}. 40% CH_3CN aqueous solution containing 1% H_3PO_4 was used as the elution solvent. The initial rates were used for the kinetic analyses. The experimental errors were within ±5% for the kinetic analyses.

Acknowledgements

This work was partly supported by a Grant-in-Aid for Scientific Research B from the Japan Society for the Promotion of Science (16370065 to S.A.).

Keywords: dehydratases · enzyme catalysis · heme proteins · metalloenzymes · mutagenesis

[1] Y. Kato, K. Nakamura, H. Sakiyama, S. G. Mayhew, Y. Asano, *Biochemistry* **2000**, *39*, 800–809.
[2] Y. Kato, Y. Asano, *Protein Expression Purif.* **2003**, *28*, 131–139.
[3] K. Kobayashi, S. Yoshioka, Y. Kato, Y. Asano, S. Aono, *J. Biol. Chem.* **2005**, *280*, 5486–5490
[4] J. Hart-Davis, P. Battioni, J. L. Boucher, D. Mansuy, *J. Am. Chem. Soc.* **1998**, *120*, 12524–12530.
[5] J. L. Boucher, M. Delaforge, D. Mansuy, *Biochemistry* **1994**, *33*, 7811–7818.
[6] K. Konishi, K. Ishida, K. Oinuma, T. Ohta, Y. Hashimoto, H. Higashibara, T. Kitagawa, M. Kobayashi, *J. Biol. Chem.* **2004**, *279*, 47619–47625.
[7] K. Konishi, T. Ohta, K. Oinuma, Y. Hashimoto, T. Kitagawa, M. Kobayashi, *Proc. Natl. Acad. Sci. USA* **2006**, *103*, 564–568.
[8] D. Barrick, *Biochemistry* **1994**, *33*, 6546–6554.
[9] G. D. DePhillis, S. M. Decatur, D. Barrick, S. G. Boxer, *J. Am. Chem. Soc.* **1994**, *116*, 6981–6982.
[10] S. M. Decatur, S. G. Boxer, *Biochemistry* **1995**, *34*, 2122–2129.
[11] S. M. Decatur, K. L. Belcher, P. K. Rickert, S. Franzen, S. G. Boxer, *Biochemistry* **1999**, *38*, 11086–11092.
[12] J. H. Dawson, A. E. Pond, M. P. Roach, *Biopolymers* **2002**, *67*, 200–206.
[13] S. Franzen, E. S. Peterson, D. Brown, J. M. Friedman, M. R. Thomas, S. G. Boxer, *Eur. J. Biochem.* **2002**, *269*, 4879–4886.
[14] M. P. Roach, S. Ozaki, Y. Watababe, *Biochemistry* **2000**, *39*, 1446–1454.
[15] M. P. Roach, W. J. Puspita, Y. Watanabe, *J. Inorg. Biochem.* **2000**, *81*, 173–182.
[16] R. Perera, M. Sono, J. A. Sigman, T. D. Pfister, Y. Lu, J. H. Dawson, *Proc. Natl. Acad. Sci. USA* **2003**, *100*, 3641–3646.
[17] A. E. Pond, M. P. Roach, M. Sono, A. H. Rux, S. Franzen, R. Hu, M. R. Thomas, A. Wilks, Y. Dou, M. Ikeda-Saito, P. R. Ortiz de Montellano, W. H. Woodruff, S. G. Boxer, J. H. Dawson, *Biochemistry* **1999**, *38*, 7601–7608.
[18] J. Sun, T. M. Loehr, A. Wilks, P. R. Ortiz de Montellano, *Biochemistry* **1994**, *33*, 13734–13740.
[19] A. Wilks, J. Sun, T. M. Loehr, P. R. Ortiz de Montellano, *J. Am. Chem. Soc.* **1995**, *117*, 2925–2926.
[20] J. Sun, M. M. Fitzgerald, D. B. Goodin, T. M. Loehr, *J. Am. Chem. Soc.* **1997**, *119*, 2064–2065.
[21] J. Hirst, S. K. Wilcox, P. A. Williams, J. Blankenship, D. E. McRee, D. B. Goodin, *Biochemistry* **2001**, *40*, 1265–1273.
[22] J. Hirst, S. K. Wilcox, J. Ai, P. Moënne-Loccoz, T. M. Loehr, D. B. Goodin, *Biochemistry* **2001**, *40*, 1274–1283.
[23] S. L. Newmyer, J. Sun, T. M. Loehr, P. R. Ortiz de Montellano, *Biochemistry* **1996**, *35*, 12788–12795.
[24] S.-X. Xie, Y. Kato, H. Komeda, S. Yoshida, Y. Asano, *Biochemistry* **2003**, *42*, 12056–12066.
[25] K. Oinuma, Y. Hashimoto, K. Konishi, M. Goda, T. Noguchi, H. Higashibata, M. Kobayashi, *J. Biol. Chem.* **2003**, *278*, 29600–29608.
[26] K. Kobayashi, B. Pal, S. Yoshioka, Y. Kato, Y. Asano, T. Kitagawa, S. Aono, *J. Inorg. Biochem.* **2006**, *100*, 1069–1074.

Received: June 27, 2006
Published online on ■■ ■■, 2006

ARTICLES

Chemical rescue of the cavity mutant of OxdB. The enzymatic activity of the H282G mutant of phenylacetaldoxime dehydratase from *Bacillus* sp. OxB-1 (OxdB) was rescued by imidazole or pyridine derivatives that acted as the exogenous proximal ligand (see scheme). By changing the electron-donation ability of the exogenous ligand with different substituents, the enzymatic activity could be regulated systematically.

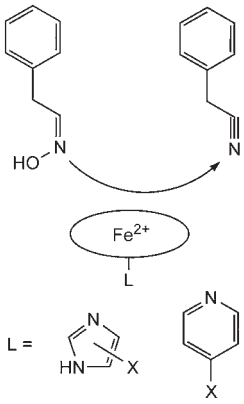

K. Kobayashi, M. Kubo, S. Yoshioka, T. Kitagawa, Y. Kato, Y. Asano, S. Aono**

■■ – ■■

Systematic Regulation of the Enzymatic Activity of Phenylacetaldoxime Dehydratase by Exogenous Ligands

